ZIBELINE INTERNATIONAL PUBLISHING

ISSN: 2521-5051 (Print)
ISSN: 2521-506X (Online)
CODEN: ASMCCQ

Acta Scientifica Malaysia (ASM)

DOI: http://doi.org/10.26480/asm.02.2020.75.81

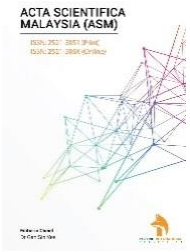

RESEARCH ARTICLE

OPTIMIZATION AND SORPTION ISOTHERMS ANALYSIS OF ANIONIC DYE EOSIN YELLOW DECONTAMINATION BY GOETHITE ADSORBENTS

Nasir Abdus-Salam, Fabian Audu Ugbe*, Abiola Victoria Ikudayisi-Ugbe

Department of Chemistry, Faculty of Physical Sciences, University of Ilorin, P.M.B. 1515, Ilorin, Nigeria.
Corresponding Author Email: ugbefabianaudu@gmail.com

ARTICLE DETAILS

Article History:

Received 04 August 2020
Accepted 10 September 2020
Available online 18 September 2020

ABSTRACT

In this work, removal of Eosin Yellow (EY) using Natural Goethite (NGT) and Synthetic Goethite (SGT) particles was studied using batch equilibrium technique. Different parameters such as initial dye concentration, particle size (NGT only), pH, and adsorbent dose were optimized to investigate the sorbents efficiency for the dye. The experimental data were tested for fitness into five common adsorption isotherm models. The various equilibrium parameters studied were found to have remarkable influence on the adsorption processes, showing optimum removal at dye concentration (150 mg/L for EY-NGT and 200 mg/L for EY-SGT), NGT particle size (0.112mm), pH (2), and dosage (0.05g), with SGT exhibiting relatively higher adsorption efficiency. The sorption data fitted well the various isotherm models in the order; Freundlich (R^2 = 0.9032) > Temkin (0.8294) > Langmuir (0.8268) > DKR (0.6431) > Flory Huggins (0.616) for EY-NGT, and Langmuir (0.9831) > Flory Huggins (0.9639) > Freundlich (0.9597) > Temkin (0.8944) > DKR (0.5993) for EY-SGT. The monolayer adsorption capacity (q_m) was calculated as 1.17 and 20.80 mgg^{-1} for NGT and SGT respectively. Additionally, combined information obtained from the isotherm study revealed that the processes were favourable, spontaneous and proceeded by a multilayer physical adsorption on already chemisorbed layer. Conclusively, the results of this study have provided useful information on the optimum working condition and mechanism of EY uptake onto goethite surfaces.

KEYWORDS

Adsorption, natural goethite, synthetic goethite, eosin yellow, isotherms.

1. INTRODUCTION

Industries make use of synthetic dyes and substantial volume of water to give a variety of products their colourful and attractive appearances (Kant, 2012). Consequently, they generate a considerable amount of contaminated wastewater (Bahramifar et al., 2015). Currently, there are over 10,000 dyes with different chemical structures available commercially (Bello et al., 2012). The presence of dyes in water even at reduced concentrations may pose severe hazard to aquatic life and constitutes human health problems such as shock, diarrhoea, jaundice, allergies, skin irritation, kidney disease, nervous disorder, genetic mutation and cancer amongst others (Zhang et al., 2020; Saini, 2017; Luo et al., 2019). Eosin yellow (EY) with chemical structure in Figure 1 is a highly water-soluble dye which causes severe skin and eye irritation (Mittal et al., 2013). It is therefore essential to carefully treat water reserves and wastewater treatment be carried out effectively.

In an effort to effectively treat dye wastewater, different techniques have been employed by many researchers such as advance oxidation, flocculation, biodegradation, photo-degradation, electrodialysis, membrane filtration, and adsorption amongst others (Zhang et al., 2020; Mohamed and Ahmed, 2017). Adsorption has proven to be one of the most promising methods, especially when using waste materials as adsorbents because of their low cost, high efficiency and ease of handling (Arunachalam et al., 2018; Anirudhan and Rajeena, 2015). Goethite, the adsorbent of choice in this study, is an iron based compound bearing OH group which enables it to attach strongly to ligands (Liu and Chen, 2013). Goethite particles are known for their high specific surface areas and strong affinities for surface binding of ions (Wang et al., 2019). Synthesized goethite has an improved purity and tailored composition with desired particle size, surface properties and colour when compared with the naturally occurring goethite (Nayak and Rao, 2005).

Many researchers have reported the removal of EY from aqueous systems using different adsorbent materials such as granular activated carbon, groundnut hull based activated carbon, Mesocellular foam silica, *Saccharomyces cerevisiae*, *Citrullus lanatus* peels, *Musanga cecropiode* saw dust, Pineapple peels, Fe_3O_4/polypyrrole, and Teak leaf litter powder amongst others (Kant, 2012; Bello et al., 2012; Li and Zhai, 2020; Bahramifar et al., 2015; Latif et al., 2019; Odiongenyi, 2020; Ugbe et al., 2018; Oyelude et al., 2017). In this study, experiment for adsorption of EY onto natural goethite (NGT) and synthetic goethite (SGT) particles was carried out in order to determine the best working conditions for adsorption of the dye in terms of initial dye concentration, dye solution pH, NGT particle size and adsorbent dosage. The study was equally focused on the adsorption isotherm modeling of experimental data to provide possible understanding of the mechanism of binding of EY onto both adsorbent surfaces.

Quick Response Code	Access this article online	
	Website: www.actascientificamalaysia.com	DOI: 10.26480/asm.02.2020.75.81

Cite the Article: Nasir Abdus-Salam, Fabian Audu Ugbe, Abiola Victoria Ikudayisi-Ugbe (2020). Optimization And Sorption Isotherms Analysis Of Anionic Dye Eosin Yellow Decontamination By Goethite Adsorbents. *Acta Scientifica Malaysia, 4(2): 75-81.*

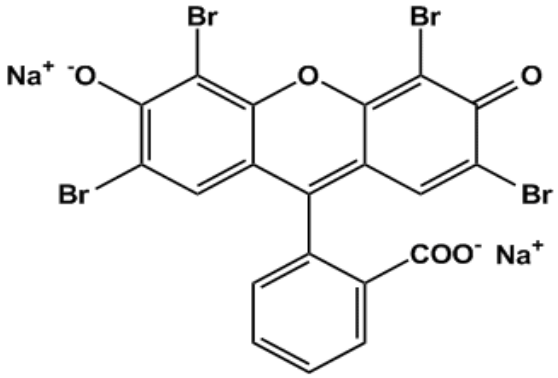

Figure 1: Chemical structure of EY

2. Materials and Methods

2.1 Adsorbent Preparation and Characterization

Fine particles of SGT (α-FeOOH) used in this study were synthesized in the laboratory according to the method reported by some researchers, while the naturally occurring goethite (NGT) was obtained from the National Iron Ore Mining Company (NIOMCO), Itakpe in Kogi State, Nigeria (Lee et al., 2004). Both Samples were then prepared and characterized using the following instrumental methods as reported; X-ray fluorescence (XRF), Fourier Transform Infrared Spectrometry (FTIR), Scanning Electron Microscopy (SEM), Brauner-Emmet-Teller Isotherm (BET), and nano-sizing technique (for SGT only) (Abdus-Salam et al., 2018). An experiment to determine the point of zero charge (pH_{pzc}) was also conducted on both adsorbents. The results of the various investigations were however published elsewhere (Abdus-Salam et al., 2018).

2.2 Optimization of Adsorption Parameters

The effects of different parameters such as initial solution concentration, adsorbent particle size, adsorbent load and pH on the uptake of EY by NGT and SGT were investigated using the batch adsorption technique. A 15 ml dye solution of varying concentrations (5, 10, 15, 25, 50, 100, 150, 200, 250 and 300 ppm) were added separately into ten (10) 100ml conical flasks each containing 0.5 g of NGT (particle size 0.112mm) and mechanically agitated on an orbital conical flask shaker for 2 hrs at 30°C. At the end of the reaction, the solutions were then filtered and the resulting filtrates analyzed for EY concentration using UV-Visible spectrophotometer at a known wavelength of maximum absorption (517nm) (Abdus-Salam and Adekola, 2005; Ladan et al., 2013). The procedure was repeated for NGT particle sizes of 0.25mm and 0.50mm, and 0.1g SGT. The optimum concentration obtained was then used as the working concentration in the subsequent experiment carried out to examine the effect of initial solution pH (2, 3, 4, 5, 6, 7 and 8) and adsorbent dosage (0.05, 0.1, 0.15, 0.20, 0.25 and 0.5g). The amounts of dye adsorbed at equilibrium were determined using equation 1 (Ugbe and Abdus-Salam, 2020).

$$q_e = \frac{V(C_i - C_e)}{m} \quad (1)$$

Where,

q_e = dye amount (mg/g) taken by the adsorbent at equilibrium
v = volume of dye solution (L)
C_i = initial dye concentration (mg/L)
C_e = equilibrium dye concentration (mg/L)
M = mass of adsorbent (g).

The experimental results were modeled using five isotherm models; Langmuir, Freundlich, Temkin, Dubinin-Kaganer-Radushkevich (DKR) and Flory-Huggins. The various equations and their parameters are presented in Table 1.

Table 1: Some adsorption isotherm equations and their parameters

Model	Equation	Linear plot	Eqn.	Author(s)
Langmuir	$\frac{C_e}{q_e} = \frac{1}{q_m}C_e + \frac{1}{K_a q_m}$ (a) $R_L = \frac{1}{1+K_a C_o}$ (b)	C_e/q_e vs C_e Slope: $1/q_m$ Intercept: $1/K_a q_m$	2	(Langmuir, 1916)
Freundlich	$logq_e = logK_F + \frac{1}{n}logC_e$	$\log q_e$ vs $\log C_e$ Slope: 1/n Intercept: $\log K_F$	3	(Freundlich, 1906)
Temkin	$q_e = BlnA + BlnC_e$ (a) $B = \frac{RT}{b}$ (b)	q_e vs lnC_e Slope: B Intercept: B*ln*A	4	(Temkin and Pyozher, 1940)
DKR	$lnq_e = lnq_d - \beta\varepsilon^2$ (a) $\varepsilon = RT\ln\left[1 + \frac{1}{C_e}\right]$ (b) $E = (-2\beta)^{-\frac{1}{2}}$ (c)	$\ln q_e$ vs ε^2 Slope: -β Intercept: *ln*q_d	5	(Al-Ahber, 2011)
Flory-Huggins	$log\left(\frac{\theta}{C}\right) = logKFH + \alpha FHlog(1-\theta)$ (a) $\theta = 1 - \frac{Ce}{Co}$ (b) $\Delta G^o = -RTlnK_{FH}$ (c)	*log*(Θ/C_o) vs *log*(1 – Θ) Slope: αFH Intercept: *log* KFH	6	(Israel and Inam, 2014)

Parameters

q_e =	ads capacity ($mg.g^{-1}$)	A =	equil ads constant (L/mg)
q_m =	monolayer ads capacity ($mg.g^{-1}$)	b =	Temkin isotherm constant relating to heat of ads (J/mol)
C_e =	equil conc (mgL^{-1})	R =	8.314 J/molK
C_o =	Initial conc (mgL^{-1})	T =	Absolute temp (K)
K_a =	Reation constant describing affinity (L/mg)	θ =	Degree of surface coverage
n =	ads intensity	K_{FH} =	Flory Huggins constant (L/mol)
K_F =	Reaction constant reflecting ads capacity (L/mg)	ΔG =	Gibb's free energy change (J/mol)
q_d =	DKR constant ($mg.g^{-1}$)	α_{FH} =	No. of analyte ions on the sorption sites
β =	Constant related to free energy (mol^2/J^2)		
ε =	Polanyi potential		
E =	Ads. Energy (J/mol)		

ads = adsorption, equil = equilibrium, temp = temperature, conc = concentration, No = number

3. Results and Discussion

3.1 Characterization

The result of characterization of the adsorbents was reported elsewhere (Abdus-Salam et al., 2018). From the results, the pH_{pzc} was reported as 7.0 and 8.0 for NGT and SGT respectively. FTIR analysis showed that the adsorbents contained majorly the hydroxyl functional group. SEM result revealed that SGT exhibited a high porosity and more regular shapes of particles than NGT. The main elemental composition of both goethite forms was Iron (Fe) with percentage composition by mass of 66.1930% and 66.4009% for NGT and SGT respectively as obtained from the XRF result. Additionally, the BET analysis revealed the SGT surface area to be 797.662 m^2/g, whilst the size of SGT particles predominantly fell into the range of 172 – 173 nm which are near nano-scale (Abdus-Salam et al., 2018).

3.2 Equilibrium Studies

3.2.1 Effect of NGT Particle Size

The uptake of EY by NGT particles of varying sizes (0.112, 0.25 and 0.50 mm) and at different solution concentrations (5 – 300 ppm) was studied for influence of variation of particle size on the adsorption. The result of this investigation is shown in Figure 2.

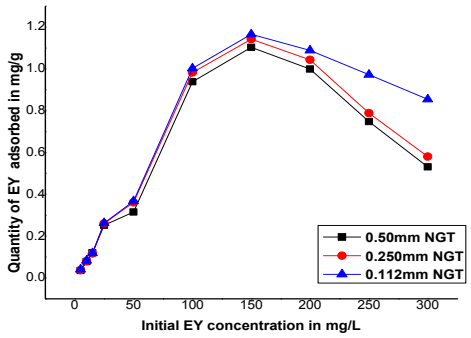

Figure 2: Effect of variation of particle size on EY adsorption at varying concentration. (Time = 2 hrs; dosage = 0.5g NGT, 0.1g SGT; temperature = 30°C)

It was observed from the curve in Figure 2 that the adsorption of EY onto NGT of varying particle sizes; 0.112mm, 0.25mm and 0.5mm essentially follow the same pattern with the 0.112mm sieve size relatively showing only a slightly higher adsorption capacity, especially as the EY solution concentration decreases. At maximum adsorption (EY conc 150 mg/L), the quantity of dye adsorbed as a function of adsorbent particle size was reported as 1.104 mg/g for 0.50mm, 1.142 mg/g for 0.25mm, and 1.166 mg/g for 0.112mm, essentially showing no significant difference. The slightly higher adsorption capacity observed for 0.112mm may however be attributed to its relatively larger surface area, and more so that diffusional resistance to mass transport is greater for adsorbent with larger particle sizes in which most of the internal surface may not be accessible or utilized for adsorption (Karthikeyan et al., 2005).

3.2.2 Effect of Initial EY Concentration

The uptake of the dye by NGT and SGT was investigated at initial concentration ranging from 5 to 300 mg/L, and the resulting curve is shown at Figure 3.

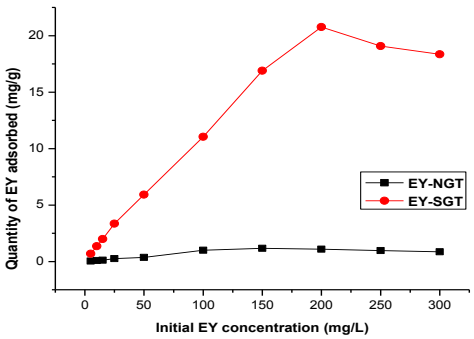

Figure 3: Effect of initial concentration on the adsorption of EY on NGT and SGT. (Time = 2hrs; NGT particle size = 0.112mm; dosage = 0.5g NGT, 0.1g SGT; NGT particle size = 0.112mm; temperature = 30°C)

From Figure 3, the amount of dye adsorbed in mg/g increases with initial dye solution concentration reaching 1.166 mg/g at 150 mg/L for EY-NGT and 20.76 mg/g at 200 mg/L for EY-SGT, after which the adsorption falls. This fall may be attributed to the saturation of the adsorption sites of the adsorbents at higher concentrations (Li and Zhai, 2020). SGT relatively exhibited greater adsorption capacity for EY removal and at higher concentration. This may be as a result of SGT containing relatively higher percent of pure goethite particles. Hence, an increased sorption sites on the surface of SGT which tends to adsorb more efficiently and reach saturation at higher concentration than the NGT. This observation is in agreement with the result reported (Abdus-Salam and Adekola, 2005). Therefore, the optimum working dye concentrations for the adsorption of EY onto both goethite forms were observed as 150 mg/L and 200 mg/L for NGT and SGT respectively.

3.2.3 Effect of Initial Solution pH

The initial pH of the dye solution is an important parameter which controls the adsorption process particularly the adsorption capacity. The pH of the solution may change the surface charge of the adsorbent, the degree of ionization of the adsorbate molecule and extent of dissociation of functional groups on the active sites of the adsorbent (Ramachandran et al., 2011). To observe the effect of pH on the extent of EY adsorption therefore, solution pH was varied from 2 – 12. The result of this study is presented in Figure 4.

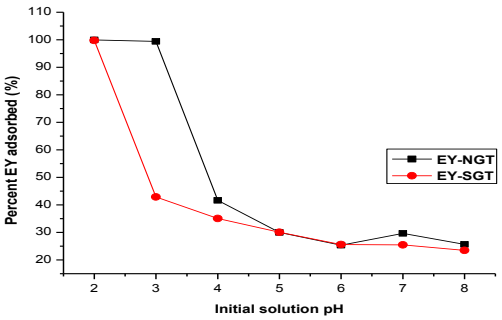

Figure 4: Effect of Initial solution pH on the sorption of EY onto NGT and SGT. (C_i = 150mg/L for NGT, 200mg/L for SGT; Time = 2 hrs; dosage = 0.5g NGT, 0.1g SGT; NGT particle size = 0.112mm; temperature = 30 °C)

The curve (Figure 4) showed there was a marked influence with a gradual rise in the uptake as pH decreases from 8 to 4 and 3 for NGT (25.62 to 41.67%) and SGT (23.46 to 42.86%) respectively. Further decrease in pH to 2 resulted to a sharp rise in the percent EY adsorbed on NGT (99.91%) and SGT (99.77%), indicating that a strong acidic medium greatly favours the adsorptive removal of EY. The adsorption process may have occurred by an electrostatic interaction in which the protonated surface of the goethite at low pH (pH < point of zero charge, pH_{pzc}) interact with the anionic groups of the dye, While at higher pH values (pH > pH_{pzc}), more OH^- ions exist and compete with the anionic groups of EY for the adsorption sites of adsorbents, thus the available adsorption sites decrease dramatically. This observation is in agreement with result obtained (Bahramifar et al., 2015; Oyelude et al., 2017). The pH range at which the surfaces of both goethites change surface charge is a function of the Point of zero charge (pH_{PZC}) of the adsorbent. The pH_{PZC} of NGT and SGT were 7.0 and 8.0 respectively as earlier reported (Abdus-Salam et al., 2018). As a result, the surface of NGT is negatively charged at pH > 7.0 and positively charged at pH < 7.0 while SGT is negatively charged at pH > 8.0 and positively charged at pH < 8.0 (Dada et al., 2020). The optimum adsorption efficiency therefore was observed at a pH of 2.

3.2.4 Effect of Variation of Adsorbent Dosage

The removal of EY at varying adsorbent loads (0.05, 1.0, 0.15, 0.20, 0.25 and 0.5 g) was studied for influence of adsorbent dosage on the adsorption efficiency. The result is as shown in Figure 5.

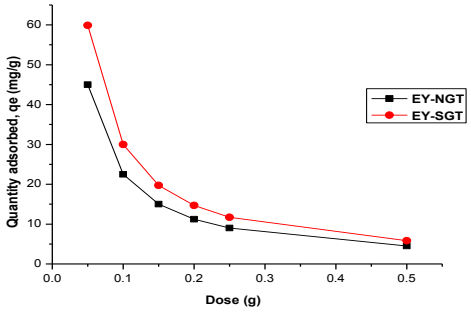

Figure 5: Effect of variation of adsorbent dosage on sorption of EY onto NGT and SGT. (C_i = 150mg/L for NGT, 200mg/L for SGT; Time = 2 hrs; pH = 2; NGT particle size = 0.112mm; temperature = 30 °C)

Result of the study showed that with increasing adsorbent load, the amount of EY adsorbed onto the unit weight of the adsorbent cuts down as shown by the declining curve of q_e versus dose (Figure 5). This may be as a result of the overlapping or aggregation of adsorption sites, leading to a decrease in overall available adsorbent surface area and an increase in diffusion path length. Similar result was reported (Bahramifar et al., 2015). Amongst the various dosages investigated, 0.05g showed the optimum adsorption capacity with 59.95 mg/g and 45.02 mg/g for SGT and NGT respectively.

3.3 Adsorption Isotherm Analysis

The data obtained from the variation of initial concentration experiment were tested for fitness into five common adsorption isotherm equations; Langmuir, Freundlich, Temkin, Dubinin-Kaganer-Raduchkevich (DKR), Temkin and Flory-Huggins. Table 2 shows the linearized isotherm parameters as obtained from the equations while the various plots were presented in Figure 6 (a-j).

Table 2: Adsorption isotherm parameters for the sorption of EY onto NGT and SGT

q_{exp} (mg/g)	Isotherm parameters									
	Langmuir		Freundlich		Temkin		DKR		Flory-Huggins	
EY-NGT										
1.17	R^2	0.8268	R^2	0.9032	R^2	0.8294	R^2	0.6431	R^2	0.616
	$K_{L(L/g)}$	0.013	$K_{F(L/mg)}$	0.021	A (L/mg)	0.214	$q_{d(mg/g)}$	1.71	K_{FH}	7096
	$q_{m(mg/g)}$	1.307	n	1.302	B (J/mol)	0.2747	$\beta_{(mol^2/J^2)}$	-8E-06	α_{FH}	11.22
	R_L	0.3390			b_o (J/mol)	9170.5	$E_{(kJ/mol)}$	0.25	$\Delta G_{(kJ/mol)}$	-22.34
EY-SGT										
20.80	R^2	0.9831	R^2	0.9597	R^2	0.8944	R^2	0.5993	R^2	0.9639
	$K_{L(L/g)}$	0.071	$K_{F(L/mg)}$	1.534	A (L/mg)	1.482	$q_{d(mg/g)}$	9.263	K_{FH}	3062
	$q_{m(mg/g)}$	20.576	n	1.769	B (J/mol)	3.584	$\beta_{(mol^2/J^2)}$	-3E-07	α_{FH}	2.314
	R_L	0.0658			b_o (J/mol)	702.89	$E_{(kJ/mol)}$	1.29	$\Delta G_{(kJ/mol)}$	-20.22

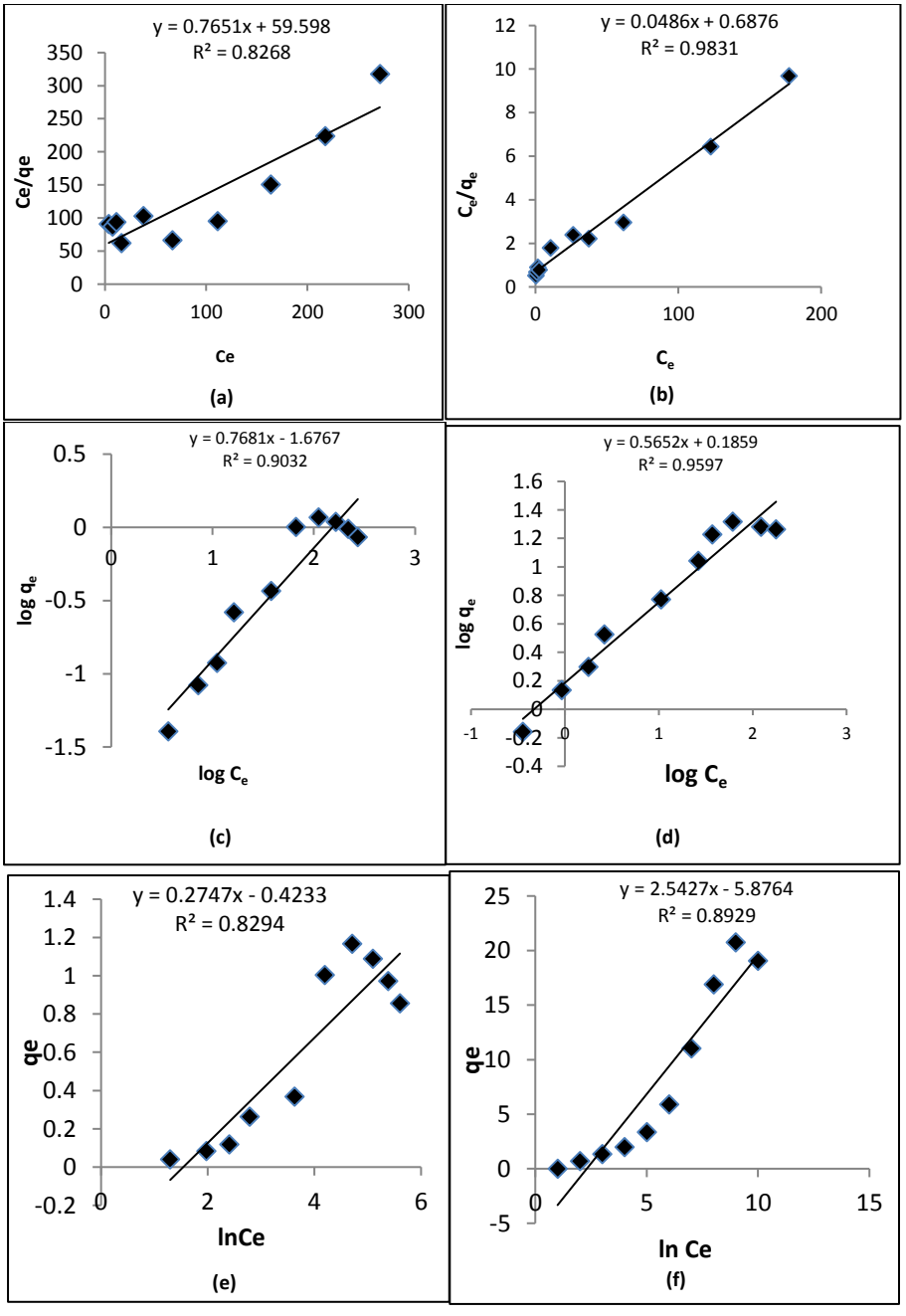

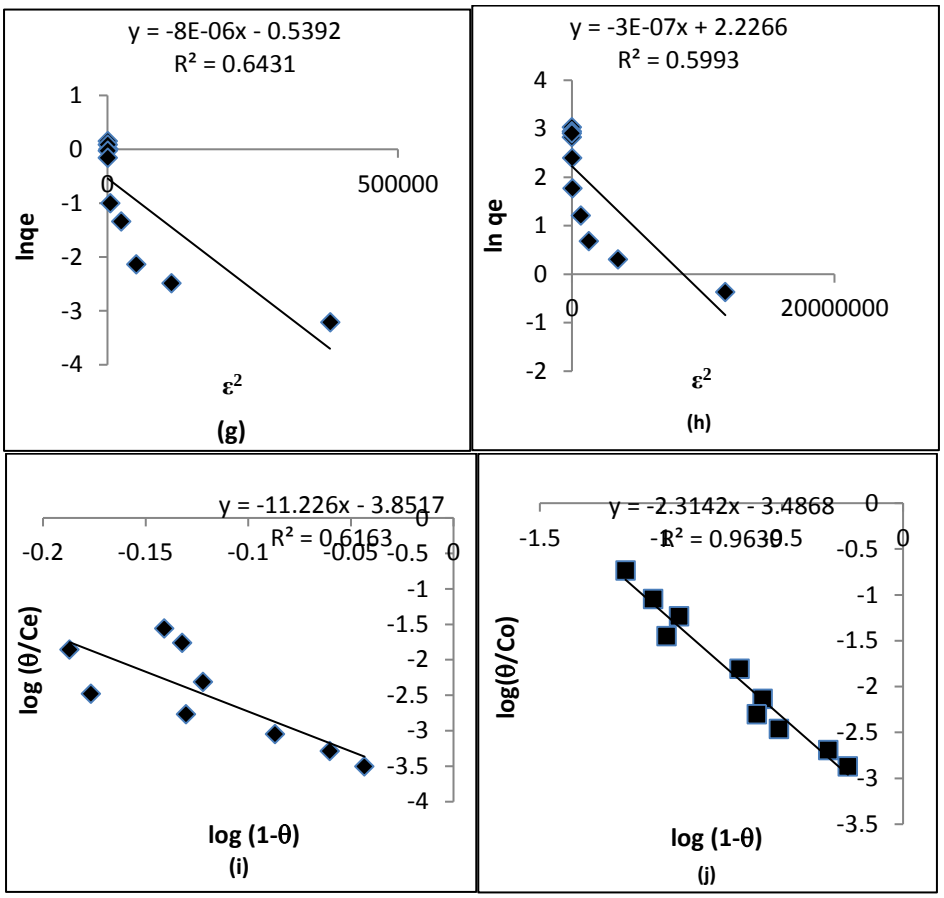

Figure 6: Adsorption isotherm plots (a) Langmuir EY-NGT (b) Langmuir EY-SGT (c) Freundlich EY-NGT (d) Freundlich EY-SGT (e) Temkin EY-NGT (f) Temkin EY-SGT (g) DKR EY-NGT (f) DKR EY-SGT (i) Flory Huggins EY-NGT (j) Flory-Huggins EY-SGT

The various values of regression coefficients (R^2) as shown in Table 2 revealed the order of fittings; Freundlich (0.9032) > Temkin (0.8294) > Langmuir (0.8268) > DKR (0.6431) > Flory Huggins (0.616) for EY-NGT, and Langmuir (0.9831) > Flory Huggins (0.9639) > Freundlich (0.9597) > Temkin (0.8944) > DKR (0.5993) for EY-SGT. Therefore, Langmuir isotherm model best fitted the adsorption process of EY onto SGT, while that of EY-NGT was best described by the Freundlich isotherm model, with the rest of other models also showing good fits in the order highlighted above.

The goodness of fit of Langmuir isotherm indicate that adsorption of EY onto both adsorbents may follow a monolayer coverage, uniform energies of adsorption onto the surface and no transmigration of the various adsorbates in the plane of the surface. Similar observation was reported (Abdus-Salam and Adekola, 2005; Boparai et al., 2010). The data generated from the adsorption experiment were subjected to the equation of separation factor, R_L in order to ascertain the favourability of the sorption process (Ugbe et al., 2018). For a favourable adsorption, $0<R_L<1$, while for an unfavourable adsorption, $R_L>1$ and when $R_L = 0$, adsorption is linear and irreversible process (Dada et al., 2012). The R_L values obtained from these adsorption processes (0.0658 for SGT and 0.3390 for NGT) are greater than zero but less than one, indicating favorability of the adsorption. To further confirm the applicability of this model to the best fitting sorption systems, a comparison between values of monolayer adsorption capacity (q_m) and the experimentally determined adsorption capacity, q_{exp} was reported in Table 2, which showed a fair closeness of the two parameters (q_m = 20.576, q_{exp} = 20.8 mg/g for EY-SGT, and q_m = 1.307, q_{exp} = 1.17 mg/g for EY-NGT). Table 3 compares the values of q_m obtained from this study with those of other adsorbents for removal of EY.

The goodness of fit of the adsorption processes of EY to Freundlich model suggests there was element of multilayer adsorption in the process mechanism. This is in agreement with results obtained (Dada et al., 2020; Boparai et al., 2010; Ugbe et al., 2018). The Freundlich exponent, *n*, should have values in the range of 1 to 10 for adsorption to be classified as favourable (Edet and Ifelebuegu, 2020). Isotherms with $n > 1$ are classified as L-type isotherms reflecting a high affinity between adsorbate and adsorbent and indicative of chemisorptions (Taha et al., 2009). As seen from Table 2, the values of n all are greater than 1, reflecting a high affinity between the dye and both adsorbents and indicative of chemisorption (Taha et al., 2009). Thus, the adsorption of EY onto NGT and SGT may proceed by multilayer adsorption on already chemisorbed layer.

The good fitting of adsorption data into the Temkin model further supports the findings that the adsorption of EY onto goethite surface may involve a chemisorption's process (Boparai et al., 2010; Ughe et al., 2018). The Temkin adsorption equilibrium binding energy constant, A which relates to the adsorptive potential of an adsorbent is greater for EY-SGT (1.482 L/mg) than for EY-NGT (0.214 L/mg). This showed that SGT has a greater adsorption potential for EY than NGT. The Temkin constant (b) related to the heat of adsorption which decreases linearly rather than logarithmically as the surface of the adsorbent is loaded due to adsorbent-adsorbate interaction, was greater for EY-NGT (9170.5 J/mol) than for EY-SGT (702.89 J/mol), suggesting a greater interaction between SGT and the dye, which corresponds to decrease in the heat of sorption of all molecules in the layer (Dada et al., 2012). This may be due to SGT containing relatively higher percent of pure goethite particles.

The DKR model assumes that the characteristic sorption curve is related to the porous structure of the adsorbent, and that the adsorption has a multi-layer character, involves Vander Waals forces and is applicable for physical adsorption processes (Yakout and Elsherif, 2010). The magnitude of the correlation coefficients, R^2 for the DKR isotherm showed that both systems, EY-NGT (0.6431) and EY-SGT (0.5993) fitted fairly well. This corroborates the multilayer and physical nature of the processes. The values of saturation capacity (q_d) of NGT and SGT were reported as 1.71 and 9.263 mg/g respectively (Table 2), indicating the porosity of SGT more than NGT. The adsorption energy, E for EY-NGT and EY-SGT were respectively 0.25 and 1.29 kJ/mol. This observation was also in agreement with results obtained (Boparai et al., 2010).

The Flory-Huggins model helps to account for the degree of surface coverage characteristic of the adsorbate on the adsorbent (Ayawei et al., 2017). The adsorption of EY onto SGT showed good fit to the Flory-Huggins model (R^2 = 0.9639) while that of EY onto NGT was only fairly modeled (R^2 = 0.616). This is indicative of good surface coverage for SGT (Israel and Inam, 2014). Also, the values of the Gibbs free energy change (ΔG) obtained from the linear plot of this model were negative (-22.34 and

-20.22 kJ/mol for EY-NGT and EY-SGT respectively), which revealed the feasibility and spontaneity of the sorption processes (Israel and Inam, 2014). In view of the isotherm study, it can be concluded that the adsorption processes of EY onto both adsorbents were favorable, spontaneous and proceeded by a multilayer physical adsorption on top of already chemisorbed layer.

Table 3: Comparison of monolayer adsorption capacities of NGT and SGT with other adsorbents for EY

Adsorbent	q_m (mg/g)	Authors
Granular activated carbon	69.638	(Kant, 2012)
Groundnut hull (activated carbon)	68.97	(Bello et al., 2012)
Mesocellular foam silica	4.003	(Li and Zhai, 2020)
Saccharomyces cerevisiae	200	(Bahramifar et al., 2015)
Citrullus lanatus peels	14.613	(Latif et al., 2019)
Musanga cecropiode saw dust	14.29	(Odiongonyi, 2020)
Pineapple peels	11.76	(Ugbe et al., 2018)
Fe_3O_4/polypyrrole	212.31	(Zhang et al., 2020)
Teak leaf litter powder	31.64	(Oyelude et al., 2017)
Natural goethite (NGT)	1.307	This study
Synthetic goethite (SGT)	20.576	This study

4. Conclusion

This study was focused on the optimization of parameters such as initial dye concentration, pH, dosage and NGT particle size, and isotherm modeling of eosin yellow (EY) adsorption onto natural goethite (NGT) and synthetic goethite (SGT) adsorbents. The dye uptake onto both adsorbents was found to be dependent on initial dye concentration, initial solution pH, adsorbent dosage, and NGT particle size. The optimum adsorption efficiencies were found in terms of the various equilibrium parameters as follows; initial dye concentration (150 mg/L for EY-NGT and 200 mg/L for EY-SGT), pH (2), dosage (0.05g), and NGT particle size (0.112mm). In all the parameters investigated, NGT could not compete favorably with SGT for adsorption of EY from aqueous solution. The experimental data fitted well tested isotherm models in the order; Freundlich (R^2 = 0.9032) > Temkin (0.8294) > Langmuir (0.8268) > DKR (0.6431) > Flory Huggins (0.616) for EY-NGT, and Langmuir (0.9831) > Flory Huggins (0.9639) > Freundlich (0.9597) > Temkin (0.8944) > DKR (0.5993) for EY-SGT. The combined results of the various isotherms showed that the processes of adsorption of EY onto both goethite forms were feasible, spontaneous, and proceeded by a multilayer physical adsorption on top of already chemisorbed layer. Therefore, this study could provide useful information on EY fixation onto goethite surfaces. For future studies, the equilibrium, kinetics and thermodynamic studies, the applicability of NGT and SGT for dyes scavenging from real industrial effluent will be tested and as comparison, a fixed bed column will be employed to investigate the effect of reactor design.

References

Abdus-Salam, N., Adekola, F.A., 2005. The influence of pH and adsorbent concentration on adsorption of lead and zinc on a natural goethite. Ife Journal of Science, 7 (1), Pp. 131 – 137.

Abdus-Salam, N., Ugbe, F.A., Funtua, M.A., 2018. Characterization of synthesized goethite and natural goethite sourced from Itakpe in North Central, Nigeria. Chem. Search Journal, 9 (2), Pp. 24 – 32.

Al-Anber, M.A., 2011. Thermodynamics approach in the adsorption of heavy metals. thermodynamics - interaction studies - solids, liquids and gases, Dr. Juan Carlos Moreno PirajÃ¡n (Eds.), Pp. 738-761.

Anirudhan, T.S., Rejeena, S.R., 2015. Photocatalytic degradation of eosin yellow using poly (pyrrole-co-aniline)-coated TiO_2/Nanocellulose composite under solar light irradiation. Journal of Materials.

Arunachalam, A., Chaudhuri, R.G., Iype, E., Kumar, B.G.P., 2018. Surface modification of date seeds (*Phoenix dactylifera*) using potassium hydroxide for wastewater treatment to remove azo dye. Water Practice and Technology, 13 (4), Pp. 860 – 870.

Ayawei, N., Ebelegi, A.N., Wankasi, D., 2017. Modelling and interpretation of adsorption isotherms. Journal of Chemistry, Pp. 1-11, retrieve from https://doi.org/10.1155/2017/3039817 on 08/07/2020.

Bahramifar, N., Tavasolli, M., Younesi, H., 2015. Removal of eosin Y and eosin B dyes from polluted water through biosorption using *Saccharomyces cerevisiae*: Isotherm, kinetic and thermodynamic studies. Journal of Applied Research in Water and Wastewater, 3, Pp. 108-114.

Bello, O.S., Fatona, T.A., Falaye, F.S., Osuolale, O.M., Njoku, V.O., 2012. Adsorption of eosin dye from aqueous solution using groundnut hull–based activated carbon: kinetic, equilibrium, and thermodynamic studies. Environmental Engineering Science, 29 (3), 186 - 194.

Boparai, H.K., Joseph, M., O'Carroll, D.M., 2010. Kinetics and thermodynamics of cadmium ion removal by adsorption onto nano zerovalent iron particles. Journal of Hazardous Materials, Pp. 1-8.

Dada, A.O., Adekola, F.A., Odebunmi, E.O., Dada, F.E., Bello, O.M., Akinyemi, B.A., Bello, O.S., Umukoro, O.G., 2020. Sustainable and low-cost Ocimum gratissimum for biosorption of indigo carmine dye: kinetics, isotherm, and thermodynamic studies. International Journal of Phytoremediation, Pp. 1-14. retrieved from https://doi.org/10.1080/15226514.2020.1785389 on 08/07/2020

Dada, A.O., Olalekan, A.P., Olatunya, A.M., Dada, O., 2012. Langmuir, Freundlich, Temkin and Dubinin–Radushkevich isotherms studies of equilibrium sorption of zn^{2+} unto phosphoric acid modified rice husk. IOSR Journal of Applied Chemistry, 3 (1), Pp. 38-45.

Edet, U.A., Ifelebuegu, A.O., 2020. Kinetics, isotherms, and thermodynamic modeling of the adsorption of phosphates from model wastewater using recycled brick waste. Processes, 8 (665), Pp. 1-15.

Freundlich, H.M.F., 1906. Over the adsorption in solution. Journal of Physical Chemistry, 57, Pp. 385–471.

Israel, A.U., Inam, E., 2014. Removal of zinc from aqueous solution by adsorption using coconut coir dust (residue and extract). Journal Chemical Society of Nigeria, 39 (1), Pp. 79-85.

Kant, R., 2012. Adsorption of dye eosin from an aqueous solution on two different samples of activated carbon by static batch method. Journal of Water Resource and Protection, 4, Pp. 93-98.

Karthikeyan, T., Sivaraman, R., Miranda, L., 2005. Chromium (VI) adsorption from aqueous solution by Hevea brasilinesis saw dust activated carbon. Journal of Hazardous Materials, 124 (1-3), Pp. 192-199.

Ladan, M., Ayuba, A.M., Bishir, U., Jamilu, A., Habibu, S., 2013. Thermodynamic properties of chromium adsorption by sediments of River Watari, Kano State. Chemsearch Journal, 4, Pp. 1 – 5.

Langmuir, I., 1916. The constitution and fundamental properties of solids and liquids. Journal of American Chemical Society, 38 (25), 2629.

Latif, S., Rehman, R., Imran, M., Iqbal, S., Kanwal, A., Mitu, L., 2019. Removal of acidic dyes from aqueous media using *citrullus lanatus* peels: an agrowaste-based adsorbent for environmental safety. Journal of Chemistry, Pp. 1-9.

Lee, G.H., Kim, S.H., Choi, B.J., Huh, S.H., 2004. Magnetic properties of needle-like α-FeOOH and γ-FeOOH nanoparticles. Journal of the Korean Physical Society, 45 (4), Pp. 1019-1024.

Li, X., Zhai, Q., 2020. Evaluation of eosin Y removal from aqueous solution using nano‐mesoporous material MCFs: adsorption equilibrium, kinetics, and adsorption isotherms. International Journal of Industrial Chemistry, retrieved from https://doi.org/10.1007/s40090-020-00202-4 on 10/07/2020.

Liu, H., Chen, T., Frost, R.L., 2013. An overview of the role of goethite surfaces in the environment, Chemosphere.

Luo, L., Wu, X., Li, Z., Zhou, Y., Chen, T., Fan, M., Zhao, W., 2019. Synthesis of activated carbon from biowaste of fir bark for methylene blue removal. R. Soc. open sci., 6.

Mittal, A., Jhare, D., Mittal, J., 2013. Adsorption of hazardous dye Eosin Yellow from aqueous solution onto waste material De-oiled Soya: Isotherm, kinetics and bulk removal. Journal of Molecular Liquids, 179, Pp. 133–140.

Mohamed, A.H., Ahmed, E., 2017. Health and environmental impacts of dyes: Mini Review. American Journal of Environmental Science and Engineering, 1 (3), Pp. 64-67.

Nayak, R., Rao, J.R., 2005. Synthesis of active goethite and maghemite from scrap iron sources. Journal of Scientific and Industrial Research, 64, Pp. 35 – 40.

Odiongenyi, A.O., 2020. Removal of eosin yellow dye from aqueous solution by adsorption onto *musanga cecrepioides* wood saw dust: experimental and theoretical study. J. Chem. Sci. Eng., 3 (2), Pp. 152-162.

Oyelude, E.O., Awudza, J.A.M., Twumasi, S.K., 2017. Equilibrium, kinetic and thermodynamic study of removal of eosin yellow from aqueous solution using teak leaf litter powder. Scientific Reports, 7, Pp. 1-10.

Ramachandran, P., Vairamuthu, R., Ponnusamy, S., 2011. Adsorption isotherms, kinetics, thermodynamics and desorption studies of reactive orange 16 on activated carbon derived from ananas comosus (L.) carbon. Journal of Engineering and Applied Sciences, 6 (11), Pp. 15-26.

Saini, R.D., 2017. Textile organic dyes: polluting effects and elimination methods from textile waste water. International Journal of Chemical Engineering Research, 9 (1), Pp. 121-136.

Taha, M.R., Ahmad, K., Aziz, A.A., Chik, Z., 2009. Geo-environmental aspects of tropical residual soils. In: B. B. K. Huat, G. S. Sew, F. H. Ali, (Eds.), Tropical Residual Soils Engineering, A. A. Balkema Publishers, London, Pp. 377-403.

Temkin, M.I., Pyozhev, V., 1940. Kinetics of ammonia synthesis on promoted iron catalyst. Acta Phys. Chim. USSR, 12, Pp. 327–356.

Ugbe, F.A., Abdus-Salam, N., 2020. Kinetics and thermodynamic modeling of natural and synthetic goethite for dyes scavenging from aqueous systems. Arab. J. Chem. Environ Res., 7, accepted for publication.

Ugbe, F.A., Anebi, P.O., Ikudayisi, V.A., 2018. Biosorption of an anionic dye, eosin yellow onto pineapple peels: isotherm and thermodynamic study. International Annals of Science, 4 (1), Pp. 14-19.

Ugbe, F.A., Funtua, M.A., Ikudayisi, A.V., 2018. Adsorption isotherms and thermodynamics study of Cd (II), Cr (III) and Cr (VI) binding by natural goethite and synthetic goethite adsorbents. Nigerian Journal of Chemical Research, 23 (2).

Wang, X., Chen, N., Zhang, L., 2019. Enhanced Cr (VI) immobilization on goethite derived from an extremely acidic environment. Environ. Sci. Nano, 6, Pp. 2185 – 2194.

Yakout, S.M., Elsherif, E., 2010. Batch kinetics, isotherm and thermodynamic studies of adsorption of strontium from aqueous solutions onto low cost rice-straw based carbons. Carbon – Science and Technology, 1, Pp. 144 –153.

Zhang, M., Yu, Z., Yu, H., 2019. Adsorption of eosin Y, methyl orange and brilliant green from aqueous solution using ferro-ferric oxide/polypyrrole magnetic composite. Polymer Bulletin, retrieved from https://doi.org/10.1007/s00289-019-02792-1 on 10/07/2020.